Graphene-based absorber exploiting guided mode resonances in one-dimensional gratings

M. Grande,[1,*] M. A. Vincenti,[2] T. Stomeo,[3] G. V. Bianco,[4] D. de Ceglia,[2] N. Aközbek,[5] V. Petruzzelli,[1] G. Bruno,[4] M. De Vittorio,[3,6] M. Scalora,[7] and A. D'Orazio[1]

[1] *Dipartimento di Ingegneria Elettrica e dell'Informazione, Politecnico di Bari, Via Re David 200, 70125 Bari, Italy*
[2] *National Research Council, Charles M. Bowden Research Center, RDECOM, Redstone Arsenal, Alabama 35898-5000 – USA*
[3] *Center for Bio-Molecular Nanotechnologies, Istituto Italiano di Tecnologia (IIT), Via Barsanti, 73010 Arnesano (Lecce), Italy*
[4] *Institute of Inorganic Methodologies and of Plasmas, IMIP-CNR, via Orabona 4, 70126 Bari, Italy*
[5] *AEgis Technologies Inc, 410 Jan Davis Dr, Huntsville - AL, 35806 USA*
[6] *National Nanotechnology Laboratory (NNL), CNR-Istituto Nanoscienze, Dip. Ingegneria dell'Innovazione, Università Del Salento, Via Arnesano, 73100 Lecce, Italy*
[7] *Charles M. Bowden Research Center, RDECOM, Redstone Arsenal, Alabama 35898-5000 – USA*
[*] *marco.grande@poliba.it*

Abstract: A one-dimensional dielectric grating, based on a simple geometry, is proposed and investigated to enhance light absorption in a monolayer graphene exploiting guided mode resonances. Numerical findings reveal that the optimized configuration is able to absorb up to 60% of the impinging light at normal incidence for both TE and TM polarizations resulting in a theoretical enhancement factor of about 26 with respect to the monolayer graphene absorption (≈2.3%). Experimental results confirm this behavior showing CVD graphene absorbance peaks up to about 40% over narrow bands of a few nanometers. The simple and flexible design points to a way to realize innovative, scalable and easy-to-fabricate graphene-based optical absorbers.

OCIS codes: (050.0050) Diffraction and gratings; (130.3120) Integrated optics devices; (300.1030) Absorption.

References and links

1. K. S. Novoselov, A. K. Geim, S. V. Morozov, D. Jiang, Y. Zhang, S. V. Dubonos, I. V. Grigorieva, and A. A. Firsov, "Electric field effect in atomically thin carbon films," Science **306**(5696), 666–669 (2004).
2. R. R. Nair, P. Blake, A. N. Grigorenko, K. S. Novoselov, T. J. Booth, T. Stauber, N. M. R. Peres, and A. K. Geim, "Fine structure constant defines visual transparency of graphene," Science **320**(5881), 1308 (2008).
3. T. Mueller, F. Xia, and P. Avouris, "Graphene photodetectors for high-speed optical communications," Nat. Photonics **4**(5), 297–301 (2010).
4. C. H. Liu, Y. C. Chang, T. B. Norris, and Z. Zhong, "Graphene photodetectors with ultra-broadband and high responsivity at room temperature," Nat. Nanotechnol. **9**(4), 273–278 (2014).
5. C.-C. Lee, S. Suzuki, W. Xie, and T. R. Schibli, "Broadband graphene electro-optic modulators with sub-wavelength thickness," Opt. Express **20**(5), 5264–5269 (2012).
6. Z. Lu and W. Zhao, "Nanoscale electro-optic modulators based on graphene-slot waveguides," J. Opt. Soc. Am. B **29**(6), 1490–1496 (2012).
7. G. Pirruccio, L. Martín Moreno, G. Lozano, and J. Gómez Rivas, "Coherent and broadband enhanced optical absorption in graphene," ACS Nano **7**(6), 4810–4817 (2013).
8. J. Liu, N. Liu, J. Li, X. J. Li, and J. Huang, "Enhanced absorption of graphene with one-dimensional photonic crystal," Appl. Phys. Lett. **101**(5), 052104 (2012).
9. X. Gan, K. F. Mak, Y. Gao, Y. You, F. Hatami, J. Hone, T. F. Heinz, and D. Englund, "Strong enhancement of light-matter interaction in graphene coupled to a photonic crystal nanocavity," Nano Lett. **12**(11), 5626–5631 (2012).
10. J. R. Piper and S. Fan, "Total absorption in a graphene monolayer in the optical regime by critical coupling with a photonic crystal guided resonance," ACS Photonics **1**(4), 347–353 (2014).

#224346 - $15.00 USD Received 7 Oct 2014; revised 11 Nov 2014; accepted 13 Nov 2014; published 12 Dec 2014

11. T. J. Echtermeyer, L. Britnell, P. K. Jasnos, A. Lombardo, R. V. Gorbachev, A. N. Grigorenko, A. K. Geim, A. C. Ferrari, and K. S. Novoselov, "Strong plasmonic enhancement of photovoltage in graphene," Nat. Commun **2**, 458 (2011).
12. M. A. Vincenti, D. de Ceglia, M. Grande, A. D'Orazio, and M. Scalora, "Nonlinear control of absorption in one-dimensional photonic crystal with graphene-based defect," Opt. Lett. **38**(18), 3550–3553 (2013).
13. A. Yu. Nikitin, F. Guinea, F. J. Garcia-Vidal, and L. Martin-Moreno, "Surface plasmon enhanced absorption and suppressed transmission in periodic arrays of graphene ribbons," Phys. Rev. B **85**(8), 081405 (2012).
14. R. Alaee, M. Farhat, C. Rockstuhl, and F. Lederer, "A perfect absorber made of a graphene micro-ribbon metamaterial," Opt. Express **20**(27), 28017–28024 (2012).
15. W. Gao, J. Shu, C. Qiu, and Q. Xu, "Excitation of plasmonic waves in graphene by guided-mode resonances," ACS Nano **6**(9), 7806–7813 (2012).
16. S. Thongrattanasiri, F. H. L. Koppens, and F. J. García de Abajo, "Complete optical absorption in periodically patterned graphene," Phys. Rev. Lett. **108**(4), 047401 (2012).
17. L. Tang, J. Du, C. Du, P. Zhu, and H. Shi, "Scaling phenomenon of graphene surface plasmon modes in grating-spacer-graphene hybrid systems," Opt. Express **22**(17), 20214–20222 (2014).
18. X. Zhu, W. Yan, P. U. Jepsen, O. Hansen, N. A. Mortensen, and S. Xiao, "Experimental observation of plasmons in a graphene monolayer resting on a two-dimensional subwavelength silicon grating," Appl. Phys. Lett. **102**(13), 131101 (2013).
19. R. Yu, R. Alaee, F. Lederer, and C. Rockstuhl, "Manipulating the interaction between localized and delocalized surface plasmon-polaritons in graphene," Phys. Rev. B **90**(8), 085409 (2014).
20. M. S. Jang, V. W. Brar, M. C. Sherrott, J. J. Lopez, L. Kim, S. Kim, M. Choi, and H. A. Atwater, "Tunable large resonant absorption in a midinfrared graphene Salisbury screen," Phys. Rev. B **90**(16), 165409 (2014).
21. B. Z. Xu, C. Q. Gu, Z. Li, and Z. Y. Niu, "A novel structure for tunable terahertz absorber based on graphene," Opt. Express **21**(20), 23803–23811 (2013).
22. A. Andryieuski and A. V. Lavrinenko, "Graphene metamaterials based tunable terahertz absorber: effective surface conductivity approach," Opt. Express **21**(7), 9144–9155 (2013).
23. J. M. Woo, M. Kim, H. W. Kim, and J. Jang, "Graphene based Salisbury screen for terahertz absorber," Appl. Phys. Lett. **104**(8), 081106 (2014).
24. R. Magnusson and S. S. Wang, "New principle for optical filters," Appl. Phys. Lett. **61**(9), 1022 (1992).
25. A. Hessel and A. A. Oliner, "A new theory of Wood's anomalies on optical gratings," Appl. Opt. **4**(10), 1275 (1965).
26. U. Fano, "Effects of Configuration interaction on intensities and phase shifts," Phys. Rev. **124**(6), 1866–1878 (1961).
27. S. Fan and J. D. Joannopoulos, "Analysis of guided resonances in photonic crystal slabs," Phys. Rev. B **65**(23), 235112 (2002).
28. E. D. Palik and G. Ghosh, *Handbook of Optical Constants of Solids* (Academic press, 1998), **3**.
29. M. Bruna and S. Borini, "Optical constants of graphene layers in the visible range," Appl. Phys. Lett. **94**(3), 031901 (2009).
30. G. W. Hanson, "Dyadic Green's functions and guided surface waves for a surface conductivity model of graphene," J. Appl. Phys. **103**(6), 064302 (2008).
31. M. Grande, M. A. Vincenti, T. Stomeo, G. Morea, R. Marani, V. Marrocco, V. Petruzzelli, A. D'Orazio, R. Cingolani, M. De Vittorio, D. de Ceglia, and M. Scalora, "Experimental demonstration of a novel bio-sensing platform via plasmonic band gap formation in gold nano-patch arrays," Opt. Express **19**(22), 21385–21395 (2011).
32. E. Hendry, P. J. Hale, J. Moger, A. K. Savchenko, and S. A. Mikhailov, "Coherent nonlinear optical response of graphene," Phys. Rev. Lett. **105**(9), 097401 (2010).
33. N. Kumar, J. Kumar, C. Gerstenkorn, R. Wang, H.-Y. Chiu, A. L. Smirl, and H. Zhao, "Third harmonic generation in graphene and few-layer graphite films," Phys. Rev. B **87**(12), 121406 (2013).
34. M. A. Vincenti, D. de Ceglia, M. Grande, A. D'Orazio, and M. Scalora, "Third-harmonic generation in one-dimensional photonic crystal with graphene-based defect," Phys. Rev. B **89**(16), 165139 (2014).

1. Introduction

Graphene is a single atomic layer of graphite that consists of very tightly bonded carbon atoms organized into a hexagonal lattice [1]. Graphene shows a sp^2 electronic configuration that leads to a total thickness of about 0.34 nm. This two-dimensional nature is responsible for the exceptional electrical, mechanical and optical properties shown by this material.

In particular, it has been theoretically and experimentally demonstrated that the absorption of a monolayer graphene does not depend on the material parameters but only on the fundamental constants since it is equal to (defined by the fine structure constant $\alpha = e^2 / \hbar c$) that corresponds to about 2.3% across the visible (VIS) range [2]. Moreover, the absorption of multiple graphene layers is proportional to the number N of added layers [2]. This important property has been exploited in different configurations to realize efficient graphene-based

#224346 - $15.00 USD Received 7 Oct 2014; revised 11 Nov 2014; accepted 13 Nov 2014; published 12 Dec 2014

photo-detectors [3,4] and modulators [5,6]. At the same time, even if this constant value is high compared with other bulk materials, the absorption of monolayer graphene can be boosted and enhanced in different spectral ranges by exploiting different technologies and approaches in both linear and nonlinear regimes. In this regard, a number of solutions have been proposed by incorporating the monolayer graphene in configurations operating in the VIS and near-infrared ranges (NIR), that exploit attenuated total reflectance (ATR) [7] or resonant configurations such as one-dimensional (1D) periodic structures [8], two-dimensional photonic crystal cavities [9], multilayer dielectric Bragg mirrors [10] or plasmonic nanostructures [11]. Within this framework, we have previously shown [12] that it is possible to achieve near perfect-absorption in a one-dimensional Photonic Crystal (PhC) that incorporates a graphene monolayer within the defect layer. Finally, enhanced absorption in monolayer graphene can also be achieved in mid-IR and terahertz (THz) ranges where this two-dimensional material shows a plasmonic behavior [13–23].

In this paper we propose and investigate a one-dimensional dielectric grating that exploits guided mode resonances (GMRs) [24] to enhance light absorption in the monolayer graphene. Guided mode resonances define optical modes with complex wavenumber, typically leaky modes, which are strongly confined in the 1D grating. Forced excitation [25] of these lattice modes may be triggered by phase-matching to incident plane waves. As a result, the interaction between these discrete modes and the out-of-plane radiation continuum gives rise to narrowband and asymmetric spectral features, also known as Fano resonances [26,27]. In this scenario, we will analyze absorption enhancement when the monolayer graphene is inserted in a lossless dielectric grating. We will numerically investigate the dependence of the absorption on the geometrical parameters with a plane wave excitation at normal incidence. Finally, we will detail the fabrication process and the experimental results related to the optical characterization of the device.

2. Numerical results

Figure 1 shows the sketch of the proposed 1D dielectric-grating-based absorber made of polymethyl-methacrylate (PMMA) stripes deposited on a tantalum pentaoxide (Ta_2O_5) slab that is supported by a silicon dioxide (SiO_2) substrate.

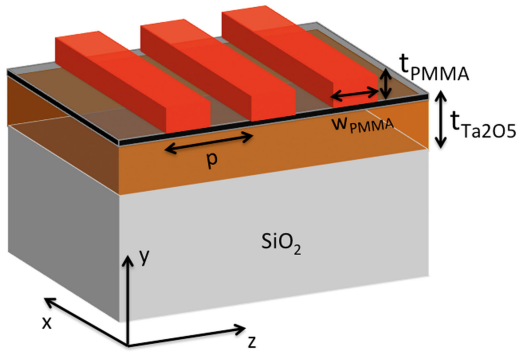

Fig. 1. Sketch of the 1D grating: PMMA stripes (red) on Ta_2O_5 slab (orange) grown on silicon dioxide substrate (grey). The black thin layer indicates the monolayer graphene.

The monolayer graphene is sandwiched between the polymeric layer and the Ta_2O_5 slab forcing it to interact with the guided mode resonances. Finally, the Ta_2O_5 slab thickness t_{Ta2O5}, the periodicity p, the PMMA width w_{PMMA} and the PMMA thickness t_{PMMA} are set initially equal to 100 nm, 470 nm, 235 nm ($w_{PMMA} = 0.6p$) and 650 nm, respectively.

The one-dimensional grating was simulated by means of the Rigorous Coupled-Wave Analysis (RCWA) in the visible-near infrared (VIS-NIR) range and the dispersion for the different dielectric media was experimentally measured by means of ellipsometric technique.

#224346 - $15.00 USD Received 7 Oct 2014; revised 11 Nov 2014; accepted 13 Nov 2014; published 12 Dec 2014

It is worth stressing that these values nearly coincide with those obtained using models based on the Sellmeier equation retrieved by the data reported in [28]. We stress that ellipsometric measurements reveal that in the range of interest the extinction coefficient is zero for the Ta_2O_5 film and approximately k_{PMMA} = 1.2e-3 for the PMMA layer. At the same time, the simulations show that the difference between the spectra with k_{PMMA} = 0 and k_{PMMA} = 1.2e-3 is less than 1% and 5% for the TE and TM polarizations, respectively, so that the device without graphene will be considered lossless hereinafter.

Finally, the monolayer graphene was modeled using the experimental fit reported in [29]. This model does not take into account the doping effect. In this respect, it is possible to refine the model following the Kubo formulation as proposed in [30], which considers the chemical potential, the temperature and the scattering time.

However, in our range of interest the variation of the complex refractive index model is negligible (a few percentage points) when the doping, i.e., the chemical potential, is varied. In contrast, the model based on the Kubo formulation is essential for describing the graphene's optical properties in the infrared and terahertz regimes. The spectral response of the configuration has been investigated for both TE and TM polarized incident plane waves. Figure 2 compares reflectance, transmittance and absorbance spectra without and with the inclusion of the monolayer graphene, respectively.

We note that the device displays two asymmetric guided mode resonances located at about 743.9 nm and 712.6 nm for TE and TM polarizations, respectively, with a full-width at half-maximum of a few nanometers. The asymmetry is evident for the transmittance and reflectance curves, while the absorption shows near-symmetric response. The spectral position satisfies the phase matching condition [25]:

$$n_{eff} = n_0 \sin\theta_{inc} - \frac{m\lambda_0}{p} \tag{1}$$

where n_{eff} corresponds to the effective refractive index of the mode in the slab, n_0 is the refractive index of cover medium, θ_{inc} is the angle of incidence of the impinging source, m is the diffraction order, λ_0 is the free space wavelength and p is the period of the grating.

At normal incidence (i.e. θ_{inc} = 0) in air (n_0 = 1) and for the first diffraction order (m = −1), Eq. (1) reduces to $n_{eff} = \lambda_0 / p$ and, hence, the free space wavelength at which the phase matching condition occurs is $\lambda_0 = n_{eff} \cdot p$.

For the configuration reported in Fig. 2, the effective refractive indices for TE and TM polarization are ~1.582 and ~1.511, respectively, leading to a guided mode resonance located at 743.5 nm and 710.2 nm. Therefore, the wavelength shift between the two polarizations (about 30 nm) is due to the different, effective refractive indices of the two modes.

Further, the plots in Fig. 2(a)-2(d) clearly prove that the introduction of the monolayer graphene enhances the absorption of the device from 2.3% up to about 50% for both polarizations; the boost in absorption is mostly due to the detriment of reflectance rather than transmittance. This behavior is due to the excitation of Fano resonances. Therefore, the graphene introduces considerable absorption in a lossless system, and leads to a slight shift and broadening of the resonances, as well as the enhancement of absorption. Finally, the field distributions for the TE (Hz component) and TM (Ez component) polarizations are shown in Figs. 2(e) and 2(f), respectively. These plots clearly show that at resonance the fields are localized at the monolayer graphene interface.

#224346 - $15.00 USD Received 7 Oct 2014; revised 11 Nov 2014; accepted 13 Nov 2014; published 12 Dec 2014

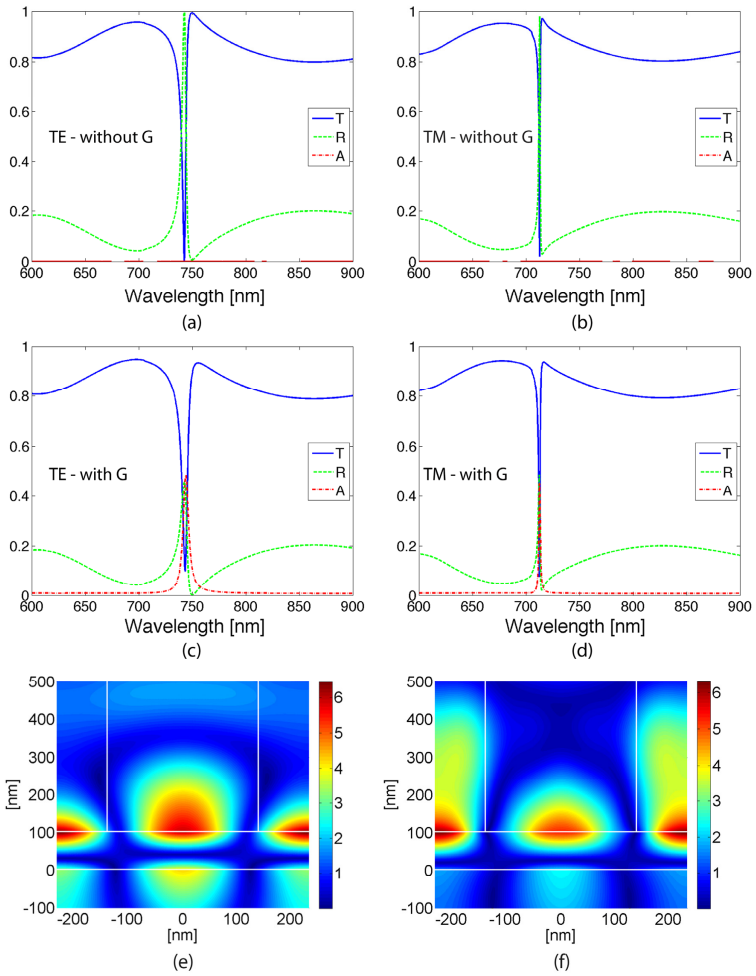

Fig. 2. Transmittance (blue solid line, T), Reflectance (green dashed curve, R) and Absorbance (red dash-dot curve, A) without (top panels) and with (bottom panels) the monolayer graphene for the TE (a-c) and TM (b-d) polarizations when t_{Ta2O5}, p, w_{PMMA} and t_{PMMA} are equal to 100 nm, 470 nm, 235 nm (0.6p) and 650 nm, respectively. Cross-section (y-z plane in Fig. 1) of the Hz (Ez) field distribution for the TE (TM) polarization ((e) and (f) respectively) when the monolayer graphene is considered (placed at 100 nm). The white lines indicate the geometry of the device.

We then proceeded to investigate the effects of technological tolerances on device performance by varying the Ta_2O_5 thickness. Figures 3(a) and 3(c) depict the absorption maps of the 1D dielectric grating for TE and TM polarizations when the Ta_2O_5 thickness t_{Ta2O5} is varied in the range 0-150 nm, leaving unchanged periodicity, fill-factor (i.e. the PMMA width) and PMMA thickness.

The maps reveal that the wavelengths associated with the guided mode resonance shift almost linearly with Ta_2O_5 slab thickness (Figs. 3(a)-3(c)). Additionally, the absorption for TM polarization shows a narrower bandwidth with respect to its TE counterpart, consistent with the spectra reported in Fig. 2. At the same time, absorption abruptly increases for both polarizations above a certain threshold because of different, effective refractive indices (Figs. 3(b)-3(d)). Above the thresholds related to the mode cutoff, absorption is rather flat for TM polarization, while it slightly increases for TE polarization. Therefore, for a Ta_2O_5 slab thickness t_{Ta2O5} = 100 nm one should be able to excite both types of guided mode resonances.

#224346 - $15.00 USD Received 7 Oct 2014; revised 11 Nov 2014; accepted 13 Nov 2014; published 12 Dec 2014

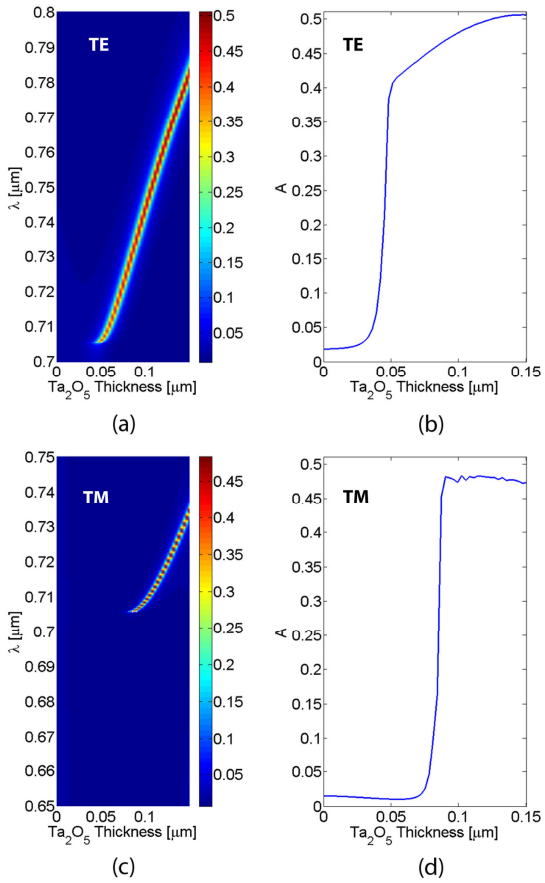

Fig. 3. Absorption maps for the (a) TE and (c) TM polarization, respectively, when the Ta_2O_5 thickness is varied. Maximum achievable absorption versus the Ta_2O_5 thickness for the (b) TE and (d) TM polarization, respectively.

A similar approach may be employed for the analysis of the optical response of the device when PMMA thickness is varied. Figure 4 depicts the behavior of the device under these circumstances. The maps in Figs. 4(a)-4(b) show that absorption is somewhat insensitive to thickness variations, while the wavelength associated with the guided mode resonance is unaffected. Consequently, the device is rather insensitive to PMMA layer thickness variations over a very large range (about 500 nm). This behavior is in agreement with the results reported in [16], confirming that an initial thickness is sufficient to excite the guided mode resonance; thus, when the thickness is increased, modal configuration is unaffected, and the optical response does not change in a noticeable way. Similar considerations may be made for reflectance spectra (Figs. 4(c)-4(d)). In conclusion, these maps indicate that the maximum attainable absorption for this configuration is about 60%, corresponding to an enhancement factor of about 26 with respect to the monolayer graphene absorption (≈2.3%).

#224346 - $15.00 USD Received 7 Oct 2014; revised 11 Nov 2014; accepted 13 Nov 2014; published 12 Dec 2014

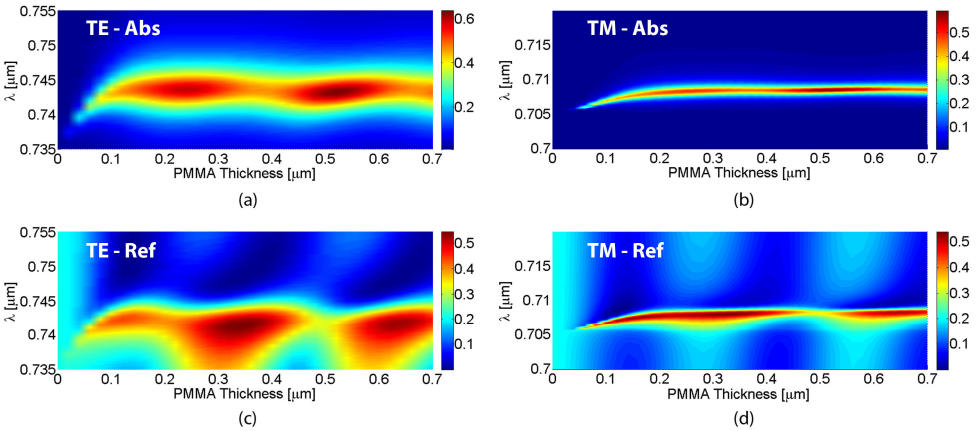

Fig. 4. Absorbance maps for the 1D dielectric grating when the PMMA thickness t_{PMMA} is varied between 0 nm and 700 nm for the (a) TE and (b) TM polarization, respectively. Panels (c) and (d) refer to the corresponding reflectance maps for the TE and TM polarization, respectively.

3. Experimental results

In order to verify the numerical findings, we fabricated the device under examination. A 100 nm-thick Ta_2O_5 slab was grown on a SiO_2 substrate by means of a RF sputtering system. The sample was treated by means of oxygen plasma in order to increase the wettability and improve the adhesion properties. Then, a monolayer graphene grown via Chemical Vapour Deposition (CVD) technique was manually transferred onto the Ta_2O_5 slab. The 1D grating was realized in two steps: first, a 650 nm-thick PMMA layer was spin-coated onto the sample, and then the PMMA layer was exposed by means of an electron beam lithography system (Raith150) operating at 20 kV. Second, the sample was developed in a methyl isobutyl ketone – isopropyl alcohol (MIBK-IPA) (MIBK-IPA) mixture and rinsed in an IPA bath.

We note that we set the PMMA thickness equal to about 650 nm since this thickness corresponds to a maximum in the reflectance maps for both polarizations, as shown in Figs. 4(c)-4(d). We retained this setting in order to verify the presence of the residual reflectance peaks.

Figure 5(a) shows the Scanning Electron Microscope (SEM) image of the final device showing the periodic PMMA stripes. The quality of the monolayer graphene was verified, after the fabrication process, by means of a Horiba Jobin-Yvon LabRAM HR-VIS micro-Raman spectrometer equipped with a 532 nm laser source.

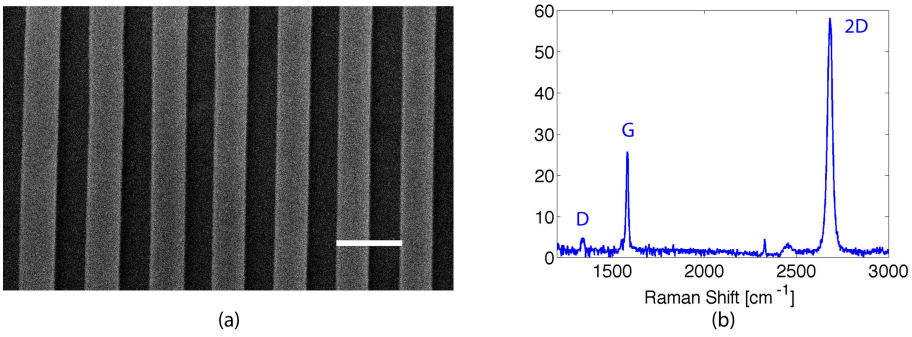

Fig. 5. (a) Scanning Electron Microscope (SEM) micrograph of the fabricated device; the white scalebar refers to 470 nm. (b) Raman spectrum of the monolayer graphene after the fabrication process.

#224346 - $15.00 USD Received 7 Oct 2014; revised 11 Nov 2014; accepted 13 Nov 2014; published 12 Dec 2014

The Raman spectrum of the processed monolayer graphene is reported in Fig. 5(b), proving the virtual absence of defects (i.e. D peak at about 1350 cm^{-1}), hence the preservation of the graphene quality.

The fabricated device was optically characterized at normal incidence by means of an setup consisting of a white-light lamp, filtered in the 600 nm–900 nm range, focused on the sample by means of a low numerical aperture, infinity-corrected microscope objective (5X, NA = 0.15) [31]. The reflected light was collected by an aspherical fiber lens collimator and filtered by a linear polarizer. An opaque metallic stage was used to support the sample and avoid collecting unwanted light. The filtered light was sent to an optical spectrometer (HR4000 from Ocean Optics) through a multimode optical fiber. The reflectance spectrum normalization was carried out by using a flat silicon surface as spectrum reference. At the same time, the transmittance spectra were collected through a perforated stage allowing the light to reach another aspherical fiber lens collimator. In this case, the Ta_2O_5 layer on the SiO_2 substrate sample was used as reference.

Figure 6 shows the comparison between theoretical and experimental results revealing excellent agreement when the periodicity p is slightly tuned by few nanometers. The experimental wavelengths for the guided mode resonances are located at about 737 nm and 695 nm, respectively and the TE polarization related peak shows a broader bandwidth (about 7 nm) with respect to the TM counterpart (about 3 nm). Furthermore, the experimental absorption is equal to 43% (34%) for TE (TM) polarization, corresponding to an enhancement factor of about 19 (15) with respect to the absorption of a monolayer graphene (equal to 2.3%).

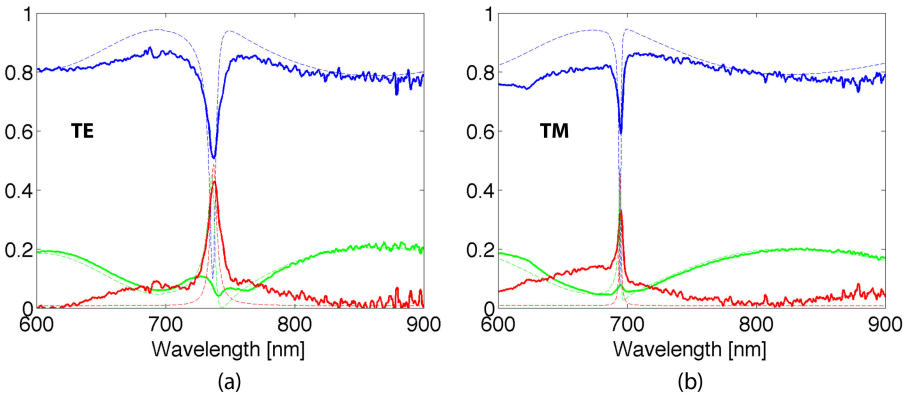

Fig. 6. Theoretical (dashed lines) and experimental (solid lines) Transmittance (blue curves), Theoretical reflectance (green curves) and Absorbance (red curves) spectra for the TE (a) and TM (b) polarizations when when t_{Ta2O5}, w_{PMMA} and t_{PMMA} are equal to 100, 235 nm (0.6p) and 650 nm, respectively.

4. Conclusion

We have detailed the design, fabrication and optical characterization of a one-dimensional dielectric grating-based absorber that incorporates a monolayer graphene and exploits polymeric stripes in order to excite guided mode resonances in the VIS-NIR range. The numerical findings reveal that a single layer of graphene suffices to absorb about 60% of the impinging light at normal incidence for both polarizations over a narrow bandwidth of a few nanometers. Further, the device is less sensitive to Ta_2O_5 slab thickness variations when this thickness exceeds a very sharp knee that defines a threshold due to the mode cutoff. Additionally, the optical response of the device is not affected even when the PMMA thickness is varied, displaying nearly flat absorption over a very large range with negligible variations.

#224346 - $15.00 USD Received 7 Oct 2014; revised 11 Nov 2014; accepted 13 Nov 2014; published 12 Dec 2014

The optical characterization revealed excellent agreement between the experimental data and the theoretical results, confirming the ability of this graphene-based absorber to achieve an enhancement factor of about 19 (15) for TE (TM) polarization. Although we have presented a 1D grating, the same idea can be extended to 2D arrays of square dielectric patches in a manner similar to that reported in [31]: this technique will enable the realization of devices that are less sensitive to the incident light polarization.

A fair comparison between our previous work reported in [12] and the proposed device allows us to draw some conclusions: the defective photonic-crystal configuration can achieve perfect absorption while the guided-mode resonance approach shows a maximum absorption of about 60%. However, the latter is based on a very simple geometry and shows low sensitivity to the geometrical parameters such as the PMMA thickness, with consequence robustness in terms of fabrication tolerances. Additionally, the proposed device requires polymeric stripes that may be easily realized using low-cost and scalable fabrication technologies, such as nano-imprinting lithography. The 1D-PhC also requires low, intrinsic dielectric losses due to the high number of layers in the dielectric stack, while presently losses depend only on two dielectric slabs. Therefore, this device could be efficiently exploited as a building block for innovative optical absorbers or photo-detectors in combination with active materials (e.g. silicon photonics based devices). Finally, the proposed solution appears also interesting in order to enhance the exceptional nonlinear third harmonic and the saturable responses of the monolayer graphene [32,33] in a fashion similar to that reported in references [12] and [34].

Acknowledgments

M. Grande thanks the U.S. Army International Technology Center Atlantic for financial support (W911NF-13-1-0434). This research was performed while the authors M. A. Vincenti and D. de Ceglia held National Research Council Research Associateship awards at the U. S. Army Aviation and Missile Research Development and Engineering Center.

#224346 - $15.00 USD Received 7 Oct 2014; revised 11 Nov 2014; accepted 13 Nov 2014; published 12 Dec 2014